Discrete element modeling and parameter calibration of vegetable plug seedling root-substrate composites

Bingliang Ye[1,2,3*], Min Jin[1], Xuefu Yu[4], Tao Tang[1,2,3], Yu Fu[1], Gaohong Yu[1,2,3]

(1. *School of Mechanical Engineering, Zhejiang Sci-Tech University, Hangzhou 310018, China*;
2. *Provincial Key Laboratory of Agricultural Intelligent Sensing and Robotics, Hangzhou 310018, China*;
3. *Key Laboratory of Agricultural Equipment for Hilly and Mountainous Areas in Southeastern China (Co-construction by Ministry and Province), Ministry of Agriculture and Rural Affairs, Hangzhou 310018, China*;
4. *Zhejiang Changshan Mingrui Electromechanical Co., Ltd, Quzhou 324200, Zhejiang, China*)

Abstract: Vegetable plug seedlings form root-substrate composites characterized by granular discreteness and cohesive bonding, which makes the direct measurement of contact parameters difficult and limits accurate simulation of transplanting processes. This study calibrated the key contact parameters and developed a discrete element method (DEM) model for broccoli plug seedling root-substrate composites by integrating physical experiments with EDEM simulations. Root shear tests, substrate angle of repose, sliding friction, and direct shear tests were performed to determine intrinsic mechanical properties. Using Plackett-Burman screening, steepest ascent, and Box-Behnken designs, the optimal combination of root static friction coefficient, critical stress, and bonding radius was obtained, with a relative error of only 0.70% between simulated and measured shear forces. For the substrate, the calibrated contact parameters of substrate-substrate and substrate-steel interactions yielded relative errors of 2.46% and 2.30%, respectively, while the simulated internal friction angle differed by only 2.64% from experimental values. The final composite model, validated through compression tests, showed a yield limit error of 4.22% and closely matched the deformation behavior observed in experiments. These results demonstrate that the proposed DEM model accurately captures the coupled mechanical behavior of flexible roots and cohesive substrates, providing a reliable tool for visual force analysis during transplanting and supporting the design optimization of seedling-picking and soil-seedling interaction mechanisms.

Keywords: vegetable plug seedling, root-substrate composites, discrete element method (DEM), contact parameter, calibration
DOI: 10.25165/j.ijabe.20261903.10320

Citation: Ye B L, Jin M, Yu X F, Tang T, Fu Y, Yu G H. Discrete element modeling and parameter calibration of vegetable plug seedling root-substrate composites. Int J Agric & Biol Eng, 2026; 19(3): 61–69.

1 Introduction

Vegetable seedling transplanting has become the dominant cultivation approach in modern vegetable production, playing a crucial role in improving crop quality and yield[1]. The establishment of mechanized transplanting systems that ensure low damage and high establishment rates requires a clear understanding of the mechanical interactions among seedlings, transplanting components, and soil. Developing a simulation platform for plug-seedling transplanting can provide valuable theoretical guidance for the optimization of transplanting mechanisms and thus promote the advancement of efficient vegetable production[2,3]. At present, research on simulation models of vegetable seedling transplanting systems and soil is relatively mature. However, there are few reports on discrete element modeling of the root-substrate composites, which are composed of roots and a mixed substrate of peat, perlite, and vermiculite, and exhibit typical discrete characteristics. During the modeling process, intrinsic physical parameters such as density, moisture content, Poisson's ratio, and elastic modulus can be determined experimentally. However, the contact parameters governing the interactions between roots and substrate particles, as well as between the composite and mechanical components, are difficult to measure directly[4-6]. Therefore, accurate calibration of these parameters is essential for constructing high-fidelity DEM models capable of reproducing the realistic mechanical behavior of plug seedlings during handling and transplanting.

Previous studies have demonstrated that combining physical experiments with discrete element simulations is an effective approach for calibrating the parameters of root-soil composites in crops such as wheat and maize, providing valuable references for this study. For instance, Li et al.[7] conducted triaxial tests and limit-equilibrium analysis on root-soil composites to investigate how root distribution angles and diameters influence shear strength parameters and root reinforcement mechanisms. Zhang et al.[8] modeled the natural state of maize stubble by adopting the Hertz-Mindlin with JKR and Bonding contact models to calibrate root-soil parameters, and developed a maize residue-soil composite model validated through shear tests. Liu et al.[9] determined the contact parameters of yam root-soil composites based on three mechanical properties and constructed a discrete element model subsequently verified through shear and compression tests, identifying morphological indices most strongly influencing maximum shear

Received date: 2025-11-11 **Accepted date:** 2026-03-31
Biographies: Min Jin, MS, research interest: intelligent agricultural equipment, Email: 1145612843@qq.com; **Xuefu Yu**, Engineer, research interest: intelligent agricultural equipment, Email: yuxuefu@vip.163.com; **Tao Tang**, PhD, research interest: intelligent agricultural equipment, Email: t.tang@zstu.edu.cn; **Yu Fu**, MS, research interest: intelligent agricultural equipment, Email: 1282927858@qq.com; **Gaohong Yu**, PhD, Professor, research interests: intelligent agricultural equipment, Email: yugh@zstu.edu.cn.
***Corresponding author: Bingliang Ye**, PhD, Professor, research interest: intelligent agricultural equipment. School of Mechanical Engineering, Zhejiang Sci-Tech University, Hangzhou 310018, China. Tel: +86-13336060776, Email: zist_ybl@zstu.edu.cn.

force. Liang et al.[10] statistically analyzed the root architectural parameters and measured the intrinsic parameters of spinach roots, establishing a high-precision discrete element model of the spinach root-soil composites that incorporates both the taproot and fibrous root systems. Parameter calibration was subsequently conducted. The results confirm that fibrous roots significantly enhance soil cohesion and stabilize the taproot, thereby improving both the visualization and simulation authenticity of the root-soil interaction process. Guo[11] established a wheat root discrete element model based on the Hertz-Mindlin with Bonding model, optimized key parameters affecting root mechanical response, and constructed a validated root-soil composites model capable of accurately reflecting field mechanical properties. In summary, although parameter calibration studies have been conducted for root-soil composites of field crops such as maize and spinach, vegetable plug-seedling composites exhibit a much looser and more cohesive structure that is prone to slippage, collapse, and rearrangement. As a result, their mechanical strength and bonding capacity are significantly reduced, and large uncertainties remain in the determination of contact parameters[12,13]. Consequently, research focusing on the calibration of contact parameters for vegetable plug-seedling root-substrate composites is still scarce, underscoring the need for further investigation.

To address this gap, the present study takes broccoli plug seedlings as the research object and combines physical testing with DEM simulations using EDEM software. Root shear tests, substrate angle of repose and sliding friction tests, and direct shear tests were performed to determine intrinsic mechanical properties and calibrate key contact parameters. Based on these calibrated parameters, a discrete element model of the root-substrate composites was developed and validated through compression experiments. The established model provides a reliable numerical foundation for simulating transplanting processes and offers theoretical support for understanding and optimizing the interactions among transplanting devices, plug seedlings, and soil.

2 Material properties

2.1 Basic characteristic parameters of plug seedling roots

To investigate the mechanical properties of plug seedling roots, broccoli plug seedlings (*Brassica oleracea* var. *italica*, cultivar Lvjian No. 3) were used as the experimental material. The seedlings were cultivated for 35 d in a greenhouse at the College of Life Sciences and Medicine, Zhejiang Sci-Tech University, as shown in Figure 1. The root system exhibits a typical taproot-fibrous-root structure, in which the taproot extends axially and fibrous roots radiate outward, forming an approximately conical three-dimensional configuration. This structure leads to pronounced anisotropic and nonlinear mechanical behavior. To quantify the geometric characteristics of the root system, a digital vernier caliper was used to repeatedly measure several morphological parameters: taproot diameter (D), basal diameter of the taproot (d), height from the fibrous-root growth node to the seedling base (L_1), distance from the fibrous-root growth node to the basal end of the taproot (L_2), and overall root spread width (L_3), as shown in Figure 2. The mean measured values were D = 1.98 mm, d = 0.98 mm, L_1 = 10.12 mm, L_2 = 15.50 mm, and L_3 = 22.64 mm, with an average fibrous-root diameter of 0.10 mm.

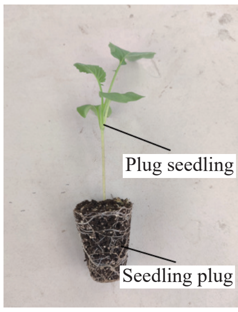

Figure 1 Broccoli plug seedling used in the experiment

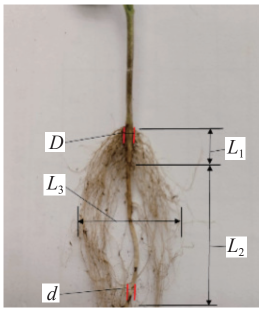

Figure 2 Schematic diagram of the broccoli root system

The root moisture content, determined using the oven-drying method, was 28.36%, and the average density was 162.24 kg/m³. Owing to significant variation in root diameter, the shear mechanical behavior exhibited a pronounced size effect. To capture this characteristic, root segments with diameters of 1.0, 1.1, 1.2, and 1.3 mm, selected according to the actual diameter distribution, were subjected to single-root shear tests using a universal testing machine at a shear rate of 1 mm/s. The results showed that the shear force increased synchronously with root diameter, indicating a size-dependent trend in the mechanical properties of the root system, as shown in Figure 3a. The shear process sequentially experienced four distinct stages: elastic deformation-linear strengthening-fiber fracture-residual friction. After reaching the peak, the shear force declined and then stabilized, as shown in Figure 3b. The calculated average peak shear force was 2.84 N, reflecting the inherent discreteness of the mechanical properties of roots.

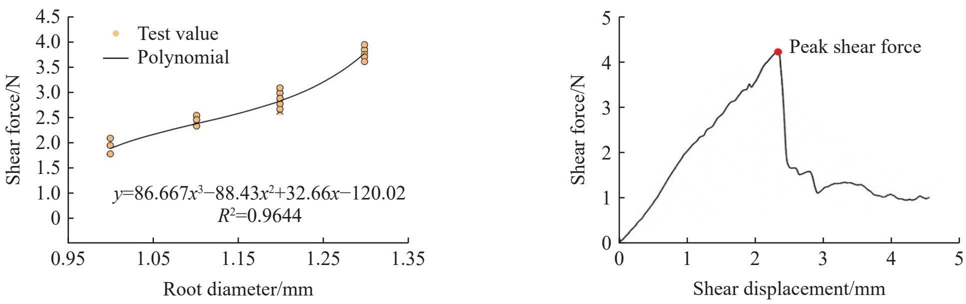

a. Relationship between peak shear force and root diameter b. Relationship between peak shear force and shear displacement

Figure 3 Shear test analysis

2.2 Basic characteristic parameters of the substrate

The plug-seedling substrate consisted of peat, vermiculite, and perlite mixed at a volumetric ratio of 3:1:1. Samples collected concurrently with the root experiments had a moisture content of 65% and a bulk density of 541.87 kg/m³. The particle-size distribution was determined using the standard sieving method (GB/T 50123-2019), and the results are summarized as listed in Table 1. The substrate showed a well-graded distribution with particle sizes ranging from 0-2.5 mm. Particles within the 0.5-1.0 mm range accounted for the highest proportion (33.66%), indicating that the substrate possessed moderate compactness and structural stability while also increasing the complexity of multiscale particle interactions during discrete element modeling.

Table 1 Particle-size distribution of the plug-seedling substrate

Particle size/mm	Mass fraction/%
>2.5	27.00
1.25-2.5	24.86
0.5-1.25	33.66
<0.5	14.48

As a typical elastoplastic medium, the angle of repose, sliding friction angle, and internal friction angle are key parameters describing the deformation and shear resistance characteristics of the substrate[14]. To evaluate its macroscopic mechanical behavior, tests were conducted to determine these parameters.

In the angle of repose test, substrate samples were poured slowly through a funnel to form a stable pile, and the angle between the slope surface and the horizontal plane was recorded as the angle of repose. In the sliding friction test, substrate samples were placed at the front end of a tilting trough, and the inclination angle was increased at a constant rate of 1 mm/s until continuous sliding occurred. The corresponding inclination angle was defined as the sliding friction angle. As listed in Table 2, the average angle of repose of the substrate was 45.19°, indicating strong interparticle friction that enhances structural stability. The average sliding friction angle between the substrate and steel was 24.35°, which reflects the frictional characteristics at external contact interfaces. This parameter directly affects the interaction mechanism between the plug substrate and the seedling-clamping claws during transplanting operations.

Table 2 Experimental results of the angle of repose and sliding friction angle of the substrate

Test group	Angle of repose/(°)	Average/(°)	Substrate-steel sliding friction angle/(°)	Average/(°)
1	45.01		23.80	
2	44.87	45.19	24.95	24.35
3	45.68		24.30	

In addition, direct shear tests were conducted using an STSJ-5A strain-controlled direct shear apparatus under normal stresses of 50 kPa, 100 kPa, 150 kPa, and 200 kPa. Shear failure was observed when the horizontal displacement reached 4 mm, as shown in Figure 4a, and the corresponding peak shear stresses were taken as the strength indices, as listed in Table 3. According to the Mohr-Coulomb failure criterion, the internal friction angle and cohesion of the substrate were determined to be 23.89° and 11.59 kPa, respectively, indicating that a certain degree of interparticle bonding existed within the substrate. Furthermore, the Poisson's ratio of the substrate was measured to be 0.37, indicating a notable tendency for lateral deformation under loading, as shown in Figure 4b.

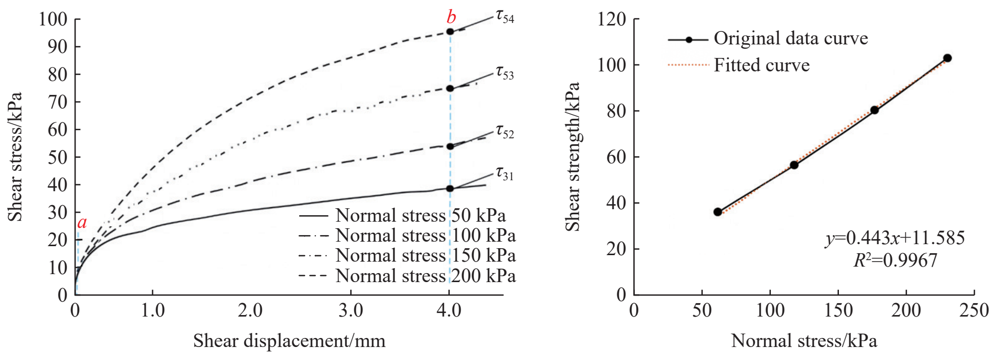

a. Direct shear test setup b. Results of the direct shear test of the substrate

Figure 4 Direct shear test analysis

Table 3 Results of the direct shear test of the substrate

Parameter	Test results			
Normal stress/kPa	50	100	150	200
Shear strength/kPa	35.14	54.53	76.55	101.64

2.3 Yield characteristic parameters of the root-substrate composites

The root-substrate composite is formed by the interlocking of roots and substrate particles. It is a typical multiphase system, whose mechanical behavior differs from that of any single component and cannot be simply regarded as a linear combination of the two. To accurately characterize its compressive properties, compression tests were performed. Because the specimens exhibited a truncated-pyramid geometry, an inclined loading platform was used to minimize edge stress concentrations during testing. The specimens were then subjected to vertical compression loading, as shown in Figure 5a. During the test, the compressive force-displacement relationship was recorded, and characteristic points were extracted through polynomial fitting, as shown in Figure 5b. The results showed that the average yield limit of the composite was 4.27 N, corresponding to a compression displacement of approximately 4 mm. This yield point represented the transition of the composite from elastic deformation to plastic failure under external loading and served as a key indicator for quantifying its overall compressive capacity. The failure mode was characterized by particle rearrangement within the substrate and progressive debonding at the root-substrate interface, revealing the complex coupled mechanical behavior of the multiphase medium.

a. Compression test of the root-substrate composite

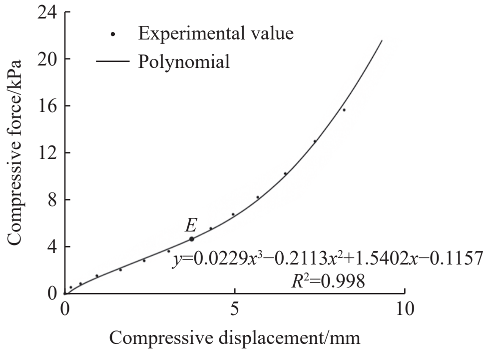

b. Compressive force-displacement curve of the root-substrate composite

Figure 5 Compression test analysis

3 Discrete element model construction and parameter calibration

3.1 Root discrete element model construction and calibration tests

The plug seedling root system can be regarded as a shear-resistant agglomerate composed of isotropic material. According to its mechanical characteristics, the Hertz-Mindlin with Bonding contact model was selected for the discrete element method (DEM) simulation of roots. Because the actual diameter of fibrous roots is extremely small, direct modeling would drastically increase the number of particles and cause computational convergence issues[15]. Therefore, the main geometric parameters of the root system were appropriately enlarged and rounded for modeling purposes: taproot diameter (D = 5 mm), basal diameter of the taproot (d = 2 mm), height from the fibrous-root growth node to the seedling base (L_1 = 10 mm), distance from the fibrous-root growth node to the basal end of the taproot (L_2 = 16 mm), overall root spread width (L_3 = 23 mm), and fibrous-root diameter = 1 mm.

On this basis, a three-dimensional geometric model of the root system was constructed in SolidWorks, and a discrete element model consistent with the actual morphology was generated using the advanced particle-filling algorithm in EDEM, as shown in Figure 6. To ensure the accuracy of parameter calibration, shear simulation tests were designed to replicate the boundary conditions of the physical experiments, as shown in Figure 7, thereby ensuring the reliability and validity of the calibration process.

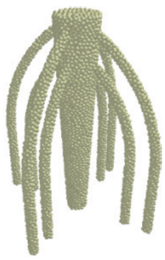

Figure 6 Three-dimensional discrete element model of the broccoli root system

3.2 Substrate discrete element model construction and calibration tests

Based on the particle-size distribution of the substrate measured in Table 1, the substrate particles were classified into four groups of non-uniform spherical particles with characteristic diameters, as listed in Table 4. Referring to the cell dimensions of a standard 128-hole plug tray (32 mm×18 mm×43 mm), a three-dimensional geometric model was constructed in SolidWorks and then imported into the EDEM platform to generate the filled assembly of non-uniform substrate particles.

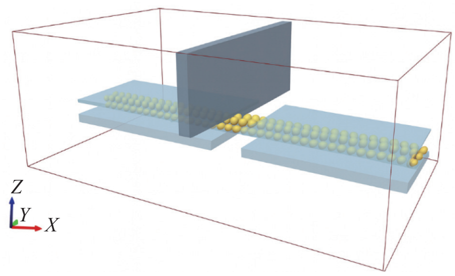

Figure 7 Shear simulation test setup and boundary conditions for parameter calibration

Table 4 Particle-size distribution of the simulated substrate particles

Actual particle size/mm	Simulated particle size/mm	Mass fraction/%	Adjusted mass fraction/%
>2.5	3	14.48	14.48
1.25-2.5	2	24.86	24.86
0.5-1.25	1	33.66	60.66
<0.5	1	27.00	

The plug-seedling substrate exhibited pronounced elastoplastic behavior during hole compression and natural settlement, accompanied by a certain degree of interparticle cohesion. To accurately characterize this property, the Hertz-Mindlin with Bonding model was employed as the contact model for substrate-substrate interactions to simulate the bonding effect between particles. Meanwhile, because substrate-steel interactions are primarily dominated by friction and collision, the Hertz-Mindlin (no slip) model was used as the contact model for substrate-steel interactions[16]. Based on the results of physical experiments and relevant literature[17], the intrinsic parameters of the substrate and 65Mn steel were determined, as listed in Table 5, and the simulation parameter ranges are summarized in Table 6.

Table 5 Intrinsic parameters of the substrate and 65Mn steel

Parameter	Substrate	65Mn steel
Poisson's ratio v_1	0.37	0.30
Shear modulus G/kPa	1×10^3	2.08×10^8
Density ρ/kg·m^{-3}	541.87	7850

Based on the internal friction angle and cohesion obtained from the direct shear test[18], the critical normal stress (σ_{max}) and critical shear stress (τ_{max}) were calculated. Because the normal stiffness coefficient (k_n) has a greater influence on the internal friction angle than the tangential stiffness coefficient (k_s), k_n was set to be one order of magnitude higher than k_s[19]. The initial bonding parameters are summarized in Table 7[20,21], where the contact radius was defined as 1.2 times the average particle radius (R = 1.065 mm).

Table 6 Simulation parameter ranges of the substrate

Interaction type	Restitution coefficient (X_1, X_4)	Static friction coefficient (X_2, X_5)	Rolling friction coefficient (X_3, X_6)
Substrate-substrate	0.15-0.55	0.20-1.16	0.02-0.05
Substrate-steel	0.20-0.50	0.50-1.20	0.02-0.05

To achieve multi-parameter collaborative calibration and model validation, the EDEM platform was used to simulate the bulk material pile angle, the material-steel friction angle, and direct shear tests, as shown in Figure 8. In the angle of repose simulation, particles were freely released from a funnel onto a receiving tray, and the angle of repose was measured once the pile reached a stable state. In the sliding friction angle simulation, particles were placed on an inclined plate that was gradually tilted at a rate of 5°/s until continuous sliding occurred, and the corresponding angle was recorded. In the direct shear simulation, a vertical load was applied via a loading plate, while the upper shear box moved relative to the lower one at a speed of 1 mm/s. The simulation was terminated when the shear displacement reached 4 mm, and the shear strength parameters were extracted for analysis.

Table 7 Bonding parameters used in the substrate contact model

Parameter	Critical normal stress/kPa	Critical shear stress/kPa	Normal stiffness coefficient/ N·m^{-3}	Tangential stiffness coefficient/ N·m^{-3}	Contact radius/ mm
Value	26.16	11.59	1×10^7	1×10^6	1.2R

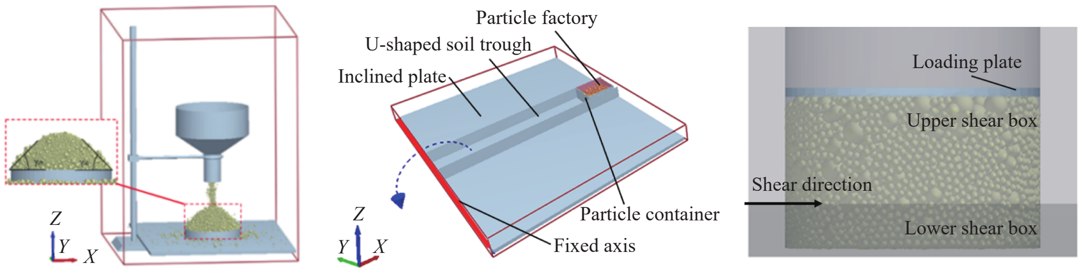

a. Angle of repose b. Sliding friction angle c. Direct shear test

Figure 8 Simulation tests of the substrate

3.3 Discrete element model construction and calibration tests of the root-substrate composites

After the independent calibration of the root and substrate contact parameters, the optimized parameters were incorporated, and the root discrete element model was combined with the substrate filling model to establish a complete discrete element model of the plug-seedling root-substrate composite. Previous studies[22] have indicated that the restitution coefficient, dynamic friction coefficient, and bonding radius of root-substrate contacts have relatively minor effects on the macroscopic mechanical response of the composite. Therefore, these factors were not selected as primary parameters for calibration in this study. To reduce the number of variables and improve calibration efficiency, the simulation parameter ranges for the root-substrate composite were defined as listed in Table 8[23].

Table 8 Simulation parameter ranges of the root-substrate composites

Restitution coefficient	Dynamic friction coefficient	Bonding radius/mm	Static friction coefficient	Bonding stiffness/ MN·m^{-3}	Critical stress/kPa
0.6	0.3	2.5	0.2-0.9	2-10	10-30

On this basis, the EDEM platform was used to conduct compression simulation tests on the root-substrate composites material, as shown in Figure 9, with the yield limit of the composites material serving as the optimization target for calibrating the contact parameters. The compression simulations effectively reproduced the overall mechanical response of the composites under external loading. By comparing the yield points and deformation patterns between the experimental and simulated results, the rationality and predictive accuracy of the established model were validated.

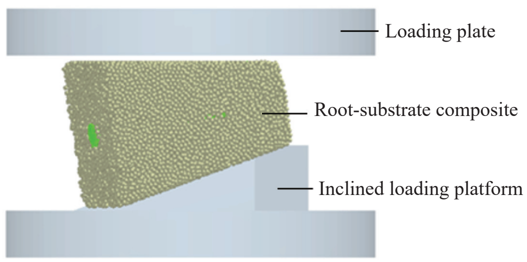

Figure 9 Compression simulation test of the root-substrate composites

4 Experimental results and analysis

4.1 Calibration results of root shear force tests

To identify the contact parameters that significantly affect the root shear force, a Plackett-Burman test was first performed, and the results were analyzed using ANOVA, as listed in Table 9. The results indicated that the static friction coefficient of roots (X_4), the critical stress (X_{10}), and the bonding radius (X_{11}) had the most significant influence on root shear force. Based on these findings, the three parameters were selected for a steepest ascent test, and the results are presented in Table 10. The parameter ranges were thereby determined as follows: static friction coefficient (X_4), 0.95-1.00; critical stress (X_{10}), 1.375-1.500 MPa; and bonding radius (X_{11}), 0.55-0.60 mm. On this basis, a Box–Behnken test was further carried out, and the results were subjected to variance analysis, as listed in Table 11. Using Design-Expert software, the data were fitted with a second-order multivariate regression model, and a predictive model for root shear force was established as follows:

$$F_{\max} = 3.05 + 0.039X_4 + 0.058X_{10} + 0.240X_{11} + 0.062X_4X_{10} - 0.050X_4X_{11} - 0.047X_{10}X_{11} - 0.055X_4^2 - 0.048X_{10}^2 + 0.045X_{11}^2 \quad (1)$$

Table 9 Analysis of variance (ANOVA) results of the Plackett-Burman test for root shear force

Parameter (root)	Code	Effect	Sum of squares	Contribution/ %	Significance ranking
Poisson's ratio	X_1	–0.12	0.04	0.21	11
Shear modulus (MPa)	X_2	–0.71	1.51	7.13	5
Restitution coefficient	X_3	0.48	0.70	3.31	8
Static friction coefficient	X_4	0.86	2.24	10.58	3
Dynamic friction	X_5	0.15	0.07	0.34	10
Root-steel restitution coefficient	X_6	–0.72	1.57	7.42	4
Root-steel static friction coefficient	X_7	–0.64	1.21	5.74	7
Root-steel dynamic friction coefficient	X_8	0.31	0.28	1.33	9
Bonding stiffness (GN·m⁻³)	X_9	–0.67	1.34	6.33	6
Critical stress (MPa)	X_{10}	0.92	2.53	11.97	2
Bonding radius (mm)	X_{11}	1.64	8.10	38.32	1

Table 10 Steepest ascent test and results for root shear force

No.	Static friction coefficient X_4	Critical stress X_{10}/MPa	Bonding radius X_{11}/mm	Peak shear force/N	Error/ %
1	0.80	1.000	0.40	0.859	–69.75
2	0.85	1.125	0.45	1.455	–48.77
3	0.90	1.250	0.50	1.983	–30.17
4	0.95	1.375	0.55	3.072	8.17
5	1.00	1.500	0.60	3.548	24.93

Table 11 ANOVA results of the Box-Behnken test for root shear force

Source of variation	Sum of squares	Degrees of freedom	Mean square	F-value	p-value
Model	0.560	9	0.062	143.76	<0.0001
X_4	0.012	1	0.012	27.80	0.0012
X_{10}	0.026	1	0.026	61.21	0.0001
X_{11}	0.460	1	0.460	1055.24	<0.0001
X_4X_{10}	0.016	1	0.016	36.16	0.0005
X_4X_{11}	0.010	1	0.010	23.14	0.0019
$X_{10}X_{11}$	0.009	1	0.009	20.88	0.0026
X_4^2	0.013	1	0.013	29.47	0.0010
X_{10}^2	0.0095	1	0.0095	21.98	0.0022
X_{11}^2	0.0085	1	0.0095	19.73	0.0030
Residual	0.0030	7	0.0004	–	–
Lack of fit	0.0030	3	0.0010	–	–
Pure error	0	4	0	–	–
Total	0.56	16	–	–	–

R^2 = 0.9946; R^2_{Adj} = 0.9877; CV = 0.69%

Adeq Precision = 37.162

Regression analysis indicated that the established second-order multivariate regression model exhibited an excellent goodness of fit (R^2=0.9946, adjusted R^2=0.9877, CV=0.69%, and *Adeq Precision*= 37.162), confirming that the model effectively described the relationship between root shear force and contact parameters. Taking the measured root shear force of 2.84 N as the optimization target, the optimal parameter combination was determined as follows: static friction coefficient of the root (X_4=0.97), critical stress (X_{10}=1.40 MPa), and bonding radius (X_{11}=0.56 mm). Using this optimized combination, multiple calibration simulations were conducted, resulting in a simulated root shear force of 2.82 N, with a relative error of only 0.70% compared to the experimental value. These results demonstrate that the developed root discrete element model accurately reproduces the shear behavior of the actual root system, and that the calibrated contact parameters are reliable for use in subsequent construction and validation of the composite model.

4.2 Calibration results of substrate angle of repose and sliding friction angle

To investigate the effects of different contact parameters on the substrate angle of repose and the sliding friction angle between the substrate and steel, a Box-Behnken experimental design was employed. The significant factors were set at three levels (low, medium, and high), and the experimental design and corresponding results are summarized in Table 12 and Table 13. The analysis of variance (ANOVA) of the experimental data is listed in Table 14 and Table 15. Using Design-Expert software, the data were fitted to a second-order multivariate regression model, and predictive equations for the substrate angle of repose (γ_α) and the substrate–steel sliding friction angle (γ_β) were established as follows:

$$\gamma_\alpha = 43.85 - 0.21X_1 + 2.02X_2 + 2.87X_3 - 0.42X_1X_2 + 1.23X_1X_3 + 0.93X_2X_3 - 0.64X_1^2 - 1.09X_2^2 - 0.81X_3^2 \quad (2)$$

$$\gamma_\beta = 22.11 - 0.22X_4 + 0.52X_5 + 1.94X_6 + 0.074X_4X_5 + 0.36X_4X_6 + 0.096X_5X_6 - 0.03X_4^2 - 0.15X_5^2 - 0.29X_6^2 \quad (3)$$

Table 12 Experimental design and results for the substrate angle of repose

No.	Restitution coefficient X_1	Static friction coefficient X_2	Rolling friction coefficient X_3	Angle of repose γ_α/(°)
1	0	–1.682	0	36.84
2	1.682	0	0	41.75
3	0	0	0	43.12
4	–1	1	–1	41.25
5	1	1	–1	37.23
6	0	0	0	43.39
7	–1	–1	–1	38.43
8	0	0	0	43.36
9	–1	–1	1	39.80
10	1	–1	1	42.38
11	1	1	1	47.24
12	0	0	1.682	47.32
13	–1	1	1	45.39
14	0	0	0	44.57
15	0	0	0	43.84
16	0	0	0	44.60
17	0	0	–1.682	36.37
18	–1.682	0	0	42.91
19	0	1.682	0	45.24
20	1	–1	1	37.06

According to the ANOVA results, the determination coefficients (R^2) of the substrate angle of repose model and the substrate-steel sliding friction angle model were 0.9685 and 0.9687, respectively, with adjusted R^2 values of 0.9401 and 0.9406. The coefficients of variation (CV) were both less than 2.0%, and the Adeq Precision values were 19.169 and 21.271, respectively, which were much higher than the threshold value of 4. These results indicate that the regression models exhibited excellent fitting accuracy and strong predictive capability.

Using the measured angle of repose of 45.19° as the optimization target, the optimal parameter combination was determined as restitution coefficient (X_1)=0.25, static friction coefficient (X_2)=0.85, and rolling friction coefficient (X_3)=0.14. Validation tests showed that the simulated angle of repose was 44.08°, with a relative error of 2.46% compared with the measured value. Similarly, taking the measured substrate–steel sliding friction angle of 24.35° as the optimization target, the optimal parameter combination was restitution coefficient (X_4)=0.42, static friction coefficient (X_5)=1.06, and rolling friction coefficient (X_6)=0.17. The corresponding simulated value was 23.79°, with a relative error of 2.30% compared with the measured value.

In summary, the optimized contact parameters for substrate-substrate and substrate–steel interactions accurately captured the piling and sliding characteristics of the substrate and provided a reliable basis for subsequent direct shear simulations and bonding parameter calibration.

Table 13 Experimental design and results for the sliding friction angle between the substrate and steel

No.	Restitution coefficient X_4	Static friction coefficient X_5	Rolling friction coefficient X_6	Sliding friction angle γ_β/(°)
1	–1	–1	–1	19.76
2	0	0	0	21.89
3	–1	–1	1	22.96
4	0	0	0	23.28
5	0	0	0	21.93
6	0	0	1.682	24.59
7	1	1	1	24.48
8	0	1.682	0	22.64
9	0	0	0	21.75
10	1	–1	1	22.91
11	1	–1	–1	18.70
12	–1	1	1	23.81
13	–1	1	–1	20.65
14	0	–1.682	0	20.86
15	0	0	0	21.72
16	1	1	–1	19.46
17	–1.682	0	0	22.50
18	1.682	0	0	21.67
19	0	0	–1.682	18.12
20	0	0	0	22.04

Table 14 Analysis of variance (ANOVA) results of the substrate angle of repose test

Source of variation	Sum of squares	Degrees of freedom	Mean square	F-value	p-value
Model	217.18	9	24.13	34.14	<0.0001
X_1	0.62	1	0.62	0.88	0.3709
X_2	55.65	1	55.65	78.72	<0.0001
X_3	112.84	1	112.84	159.63	<0.0001
X_1X_2	1.43	1	1.43	2.02	0.1856
X_1X_3	12.05	1	12.05	17.05	0.002
X_2X_3	6.96	1	6.96	9.84	0.0106
X_1^2	5.88	1	5.88	8.32	0.0163
X_2^2	17.28	1	17.28	24.44	0.0006
X_3^2	9.46	1	9.46	13.88	0.0044
Residual	7.07	10	0.71	–	–
Lack of fit	5.09	5	1.02	2.57	0.1619
Pure error	1.98	5	0.40	–	–
Total	224.25	19	–	–	–

R^2 = 0.9685; R^2_{Adj} = 0.9401; CV = 2.00%;
Adeq Precision = 19.169

Table 15 ANOVA results of the sliding friction angle test between substrate and steel

Source of variation	Sum of squares	Degrees of freedom	Mean square	F-value	p-value
Model	58.19	9	6.47	34.41	<0.0001
X_4	0.67	1	0.67	3.57	0.0882
X_5	3.65	1	3.65	19.44	0.0013
X_6	51.31	1	51.31	273.08	<0.0001
X_4X_5	0.044	1	0.044	0.23	0.6407
X_4X_6	1.03	1	1.03	5.48	0.0413
X_5X_6	0.074	1	0.074	0.39	0.5441
X_4^2	0.013	1	0.013	0.071	0.7954
X_5^2	0.32	1	0.32	1.70	0.2216
X_6^2	1.20	1	1.2	6.38	0.0300
Residual	1.88	10	0.19	–	–
Lack of fit	0.14	5	0.029	0.082	0.9920
Pure error	1.74	5	0.35	–	–
Total	60.07	19	–	–	–

R^2 = 0.9687; R^2_{Adj} = 0.9406; CV = 1.99%;
Adeq Precision = 21.271

4.3 Calibration results of the substrate direct shear test

Using the measured internal friction angle of 23.89° as the optimization target, a series of simulation tests were conducted by iteratively adjusting the normal and tangential stiffness coefficients. The results showed that when the normal stiffness coefficient was 5×10^7 N/m³ and the tangential stiffness coefficient was 5×10^6 N/m³, the simulated internal friction angle of the substrate was 23.26°, with a relative error of 2.64% compared with the measured value. A comparison of the bonding state of the substrate in the simulation and experiment at the end of shearing is presented in Figure 10.

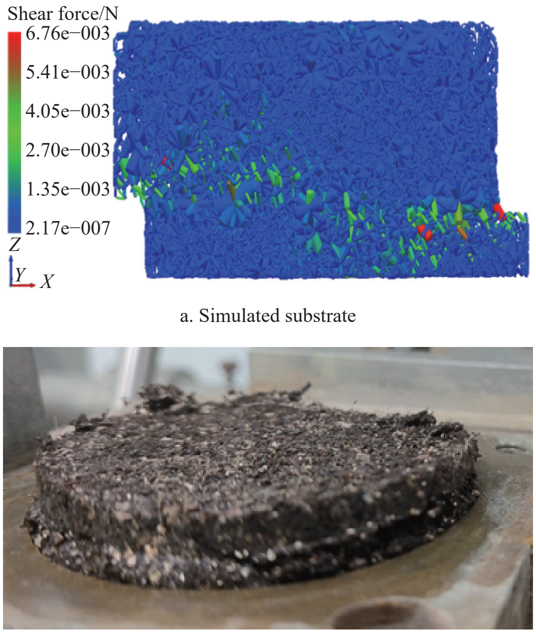

a. Simulated substrate

b. Physical substrate

Figure 10 Bonding state of the simulated versus actual substrate at the end of shearing

As the shear progressed to the final stage, the shear stress along the shear plane displayed a distinctly nonlinear distribution. The bonding contacts at the external surfaces experienced extensive breakage, while those between internal particles underwent sliding, collapse, and rearrangement, eventually forming staggered fracture zones above and below the shear plane, as shown in Figure 10a. As shown in Figure 10b, the morphology of the simulated fracture zone is highly consistent with that observed in the physical direct shear test, confirming that the calibrated contact parameters can effectively reflect the shear resistance of the substrate. These results verify that the developed discrete element model exhibits high reliability in reproducing the shear behavior of the substrate.

4.4 Calibration results of root-substrate composites compression tests

To further calibrate the key contact parameters of the root-substrate composites, the steepest ascent method was employed to perform compression simulations under different parameter combinations. The experimental design and corresponding results are summarized in Table 16.

Table 16 Experimental design and results of the steepest ascent test for root-substrate composites compression

No.	Static friction coefficient	Bonding stiffness/ MN·m^{-3}	Critical stress/kPa	Yield limit/N	Error/ %
1	0.2	2	10.0	1.78	–58.31
2	0.3	3	12.5	2.06	–51.76
3	0.4	4	15.0	2.40	–43.79
4	0.5	5	17.5	2.71	–36.53
5	0.6	6	20.0	3.29	–22.95
6	0.7	7	22.5	3.67	–14.05
7	0.8	8	25.0	4.34	1.64
8	0.9	9	27.5	4.48	4.92
9	1.0	10	30.0	4.63	8.43

The results showed that with the gradual increase in static friction coefficient, bonding stiffness, and critical stress, the simulated yield limit of the composite exhibited a progressive upward trend, approaching the experimentally measured value of 4.27 N. Among all parameter combinations, condition 7 (static friction coefficient = 0.8, bonding stiffness = 8 MN/m^3, and critical stress = 25 kPa) yielded the best agreement with the experimental result, producing a simulated yield limit of 4.34 N and a relative error of only 1.64%. This result was markedly superior to those obtained under other parameter combinations. Therefore, the optimal contact parameters between the root and substrate particles were determined to be a static friction coefficient of 0.8, a bonding stiffness of 8 MN/m^3, and a critical stress of 25 kPa. These findings confirm that the developed discrete element model accurately reproduces the macroscopic yield characteristics of the root-substrate composite under compression and provides reliable parameter support for subsequent numerical simulations of the transplanting process.

5 Validation and analysis of the root-substrate composites discrete element model

To verify the reliability of the constructed discrete element model, compression simulations of the broccoli plug seedling root-substrate composites were conducted using the calibrated and optimized contact parameters. The simulation results were then compared with those obtained from physical compression tests.

The results showed that the simulated yield limit of the composite was 4.45 N, whereas the measured value was 4.27 N, corresponding to a relative error of 4.22%, which is well below the engineering tolerance threshold of 7%[24]. Combined with the comparative analysis of the force-displacement curves shown in Figure 11, it can be seen that the simulated and experimental curves exhibit a high degree of agreement in variation trend throughout the entire compression process. The compression process can be divided into three stages: initial compression, linear elasticity, and plastic yielding. During the initial compression stage (O-D/D′), due to the rough surface and loose internal structure of the composite, multiple point contacts formed between the specimen and the loading plates. Consequently, the compressive force in both the simulation and experiment increased gradually with displacement, and the relative error in force between them was the smallest in this stage. The compression process entered the linear elastic stage (D-E/D′-E′), during which the contact mode gradually transitioned from point contact to surface contact. Both the simulation and experimental curves exhibited a linear relationship, confirming that the model accurately captures the mechanical behavior of the composite in the elastic stage. When the compression reached the yield points (E /E′), the composite entered the plastic yielding stage. At this point, rearrangement of substrate particles and slip at the root-substrate interface occurred. Consequently, the slopes of both the simulation and experimental curves increased significantly, demonstrating typical compaction-hardening behavior accompanied by irreversible plastic deformation.

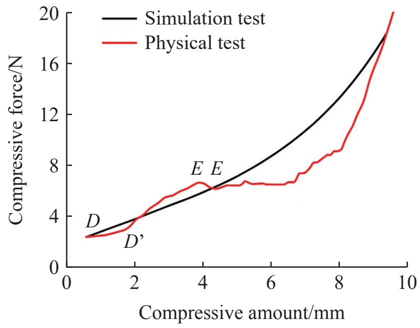

Figure 11 Comparison between simulated and experimental compression force-displacement curves

To validate the model's robustness under dynamic loads, a drop simulation test was further conducted on the plug seedling root-substrate composite, presented in Figure 12. The results showed that after free fall, the overall composite structure remained intact, with only minor shedding of substrate particles and no significant collapse or delamination observed. These findings indicate that the model can reasonably represent the mechanical response of the plug seedling under impact loading. Simultaneously, the test verifies the stability and predictive reliability of the composite model under dynamic operating conditions, demonstrating its favorable impact resistance and low-loss characteristics. In summary, the systematically calibrated discrete element model of the root-substrate composite accurately reproduced the mechanical response and deformation evolution of plug seedlings under various loading conditions, exhibiting excellent engineering applicability and numerical reliability. The model provides a robust numerical

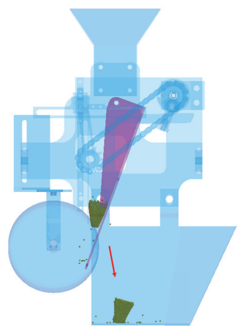

Figure 12 Drop simulation test of the root-substrate composites

foundation for simulating the interaction between transplanting mechanisms and plug seedlings, serving as an effective computational platform and theoretical tool for elucidating the interaction mechanisms within the "transplanting mechanism-plug seedling-soil" system, analyzing seedling damage mechanisms, and optimizing low-damage transplanting designs.

6 Conclusions

This study investigated the mechanical properties and interaction mechanisms of broccoli plug seedling roots, substrate, and their composites by combining physical experiments with discrete element simulations. Combining the Hertz-Mindlin with Bonding contact model with a multi-step optimization strategy, including the Plackett-Burman design, the steepest ascent method, and Box-Behnken design, the key parameters at the root-substrate interface were systematically calibrated. These parameters were used to develop a highly accurate and reliable discrete element model of the root-substrate composites, which effectively reproduced the macroscopic mechanical behavior and deformation characteristics of plug seedlings.

1) Through root shear tests and discrete element simulations, the static friction coefficient, critical stress, and bonding radius were identified as the most influential parameters affecting root shear resistance. The optimal combination (0.97, 1.4 MPa, and 0.56 mm) yielded a simulated shear force with only 0.70% relative error, indicating the model's strong predictive capability for root mechanical response.

2) Angle of repose tests and simulations revealed that restitution coefficient, static friction coefficient, and rolling friction coefficient were the dominant factors. The optimal parameter set (0.25, 0.85, 0.14) produced a simulated repose angle of 44.08°, differing from the measured value by only 2.46%, confirming that the model effectively represents the substrate's macroscopic flow behavior.

3) Based on sliding friction tests, the key parameters—restitution coefficient, static friction coefficient, and rolling friction coefficient—were optimized to (0.42, 1.06, 0.17). The simulated sliding friction angle differed by only 2.30% from the experimental value, validating the model's high accuracy in capturing substrate–steel contact properties.

4) By optimizing normal and tangential stiffness coefficients to 5×10^7 N/m^3 and 5×10^6 N/m^3, respectively, the simulated internal friction angle reached 23.26°, with a relative error of 2.64%, demonstrating that the model accurately reproduces the substrate's shear deformation characteristics.

5) Using the optimized parameters, a discrete element model of the root-substrate composites was developed. Compression simulations showed a yield limit of 4.34 N, closely matching the experimental value of 4.27 N (error 4.22%). The simulated deformation and failure morphology were consistent with physical observations, confirming the model's robustness and predictive reliability.

Acknowledgements

This study was financially supported by Zhejiang Provincial Natural Science Foundation of China (Grant No. LD24E050007) and the National Natural Science Foundation of China (Grant No. 32171899). Any opinions, findings, conclusions, or recommendations expressed in this publication are those of the authors and do not necessarily reflect the view of Zhejiang Sci-Tech University.

[References]

[1] Yu G H, Wang L, Sun L, Zhao X, Ye B L. Research progress on mechanized transplanting technology and equipment for field crops. Transactions of the CSAM, 2022; 53(9): 1–20. (in Chinese)

[2] Bai H B, Zeng F D, Su Q, Cui J, Li X Y. Study on the interaction characteristics between pot seedling and planter based on hanging cup transplanter. Sci Rep., 2025; 15: 10031.

[3] El Salem A, Shang S Q, Wang D W, Zhang G Z, Wang H C, Abdeen M A, et al. Developing an adequate DEM model to simulate soil-tool interactions under sticky soil conditions. Soil Tillage Res., 2026; 256: 106893.

[4] Zeng Z W, Ma X, Cao X L, Li Z H, Wang X C. Application status and prospects of the discrete element method in agricultural engineering research. Transactions of the CSAM, 2021; 52(4): 1–20. (in Chinese)

[5] Zhang S L, Yang F F, Dong J X, Chen X H, Liu Y, Mi G P, et al. Calibration of discrete element parameters of maize root and its mixture with soil. Processes, 2022; 10(11): 2433.

[6] Zhou H L, Yang W, Yu G H, Wang B, Ye B L. Optimization design and experiment of a multi-link transplanting mechanism with ditching for vegetable plug seedlings. Transactions of the CSAM, 2023; 54(3): 79–85. (in Chinese)

[7] Li P C, Xiao X P, Wu L Z, Li X, Zhang H, Zhou J T. Study on the shear strength of root-soil composite and root reinforcement mechanism. Forests, 2022; 13(6): 898.

[8] Zhang S L, Zhao H B, Wang X Z, Dong J X, Zhao P F, Yang F F, et al. Discrete element modeling and shear properties of the maize stubble-soil complex. Comput Electron Agric., 2023; 204: 107519.

[9] Liu Y G, Zhao J G, Yin B Z, Ma Z K, Hao J J, Yang X, et al. Discrete element modelling of the yam root-soil complex and its verification. Biosyst Eng., 2022; 220: 55–72.

[10] Liang S J, Liu L J, Liu F J, Chang H, Cui W, Li G L. Establishment and calibration tests of a discrete element model for spinach root-soil composite. Transactions of the CSAE, 2025; 41(5): 38–49. (in Chinese)

[11] Guo C C. Parameter optimization research of cross-slot opener based on discrete element model of root-soil composite. PhD dissertation. Yangling: Northwest A&F University, 2021. Doi: 10.27409/d.cnki.gxbnu.2021.002218. (in Chinese)

[12] Mak J, Chen Y, Sadek M A. Determining parameters of a discrete element model for soil-tool interaction. Soil Tillage Res., 2012; 118: 117–122.

[13] Wang X Q, Zhou H L, Tong J H. Shear characteristics of root-matrix composites under various interface friction and moisture content conditions. Rhizosphere, 2024; 31: 100944.

[14] Zhu L T, Liao Q X, Wang Z T, Chen J, Chen Z L, Bian Q W, et al. Prediction of soil shear strength parameters using combined data and different machine learning models. App.Sci., 2022; 12(10): 5100.

[15] Kafashan J, Kafashan J, Wiącek J, Rahman N A, Gan J Q. Two-dimensional particle shapes modelling for DEM simulations in engineering: A review. Granul Matter, 2019; 21(3): 80.

[16] Franco Y, Rubinstein D, Shmulevich I. Prediction of soil-bulldozer blade interaction using discrete element method. Transactions of the ASABE, 2007; 50(2): 345–353.

[17] Zdancevičius E, Kačianauskas R, Zabulionis D. Improvement of viscoelastic damping for the Hertz contact of particles due to impact velocity. Procedia Eng., 2017; 172: 1286–1290.

[18] Wang X L, Hu H, Wang Q J, Li H W, He J, Chen W Z. Calibration method of soil model parameters based on DEM. Transactions of the CSAM, 2017; 48(12): 78–85. (in Chinese)

[19] Ai J, Chen J F, Rotter J M, Ooi J Y. Assessment of rolling resistance models in discrete element simulations. Powder Technol., 2011; 206(3): 269–282.

[20] Ucgul M, Saunders C, Li P L, Lee S-H, Desbiolles J M A. Analyzing the mixing performance of a rotary spader using digital image processing and discrete element modelling (DEM). Comput Electron Agric., 2018; 151: 1–10.

[21] Bahrami M, Naderi-Boldaji M, Ghanbarian D, Ucgul M, Keller T. Simulation of plate sinkage in soil using discrete element modelling: Calibration of model parameters and experimental validation. Soil Tillage Res., 2020; 203: 104700.

[22] Sun J. Structural and mechanical properties of maize stubble and its tribological performance with soil. Changchun: Jilin University, 2011. (in Chinese)

[23] Potyondy D, Cundall P. A bonded-particle model for rock. Int J Rock Mech Min Sci., 2004; 41: 1329–1364.

[24] Barr J, Ucgul M, Desbiolles J, Fielke J. Simulating the effect of rake angle on narrow opener performance with the discrete element method. Biosyst Eng., 2018; 171: 1–15.